RSC Advances

PAPER

View Article Online
View Journal | View Issue

Cite this: *RSC Adv.*, 2026, **16**, 27906

Oxidovanadium(v) coordination compounds based on 1,5-bis(2-hydroxy-3-methoxybenzylidene) carbohydrazide: from discrete to polymeric assemblies

Diana Dragancea, *[a] Natalia Talmaci, [b] Sergiu Shova, [c] Anamaria Hanganu, [a] Simon Grabowsky, [d] Silvio Decurtins, [e] Shi-Xia Liu [e] and Svetlana G. Baca *[f]

The reaction of NH_4VO_3 or $VO(acac)_2$ with 1,5-bis(2-hydroxy-3-methoxybenzylidene)carbohydrazide (H_4L) has led to the formation of new homometallic dinuclear and tetranuclear V(v) coordination compounds, namely $(NH_4)_2[(VO_2)_2(L)]\cdot 2H_2O$ (**1**) and $[(VO_2)(VO)(EtO)(HL)]_2\cdot 2EtOH$ (**2**). The introduction of alkali metal cations (Na^+ and Cs^+) into the reaction resulted in the formation of the heterometallic hexanuclear $[Na_2(H_2O)_4][(VO_2)_4(HL)_2]\cdot 16H_2O$ compound **3** and the $\{[Cs_2(H_2O)_2][(VO_2)_2(L)]\}_n$ coordination polymer **4**. Their composition and structure were determined by IR, ^1H and ^{13}C NMR spectroscopy, and ESI-MS spectrometry. Single-crystal X-ray diffraction analysis of **1** reveals that the hexadentate L^{4-} ligand coordinates to two V(v) atoms *via* an ONN and an ONO donor set, resulting in the formation of a dinuclear vanadium-based complex dianion, $[(VO_2)_2(L)]^{2-}$. The charge is compensated by two NH_4^+ cations. In **2**, two dinuclear vanadium-based $[(VO_2)(VO)(EtO)(HL)]$ entities, each containing the hexadentate Schiff base ligand HL^{3-}, which utilizes a set of donor atoms in a manner analogous to that in **1**, are bridged through oxido (V–O–V) bonds into a tetranuclear cluster. In compound **3**, the hexadentate HL^{3-} utilizes additional donor atoms to bind sodium cations to two $[(VO_2)_2(HL)]^-$ moieties. The $[Na_2(H_2O)_4]^{2+}$ cations are sandwiched by the oxygen atoms of the methoxy groups of the HL^{3-} ligands and the oxide atoms of the VO_2 core resulting in the formation of a hexanuclear cluster in **3**. The structure of compound **4** is based on the mutually linked clusters containing monomeric $[(VO_2)_2(L)]^{2-}$ moieties and water-alkali chains $\{[Cs_2(H_2O)_2]\}_n$ to form a 3D coordination framework.

Received 27th March 2026
Accepted 28th April 2026

DOI: 10.1039/d6ra02540d

rsc.li/rsc-advances

Introduction

Vanadium compounds play a significant role in processes related to living organisms and the environment. For example, vanadate-containing haloperoxidases found in algae and certain bacterial species are well-documented,[1–9] while other vanadium-containing enzymes are capable of fixing nitrogen.[10–12] The metabolism of these bacteria involves the conversion of vanadate into oxidovanadium(IV). In addition, vanadium complexes catalyse oxidation reactions in industrial processes[13–16] and are used in the production of high-capacity lithium vanadate batteries, supercapacitors, energy-saving smart windows, optoelectronic devices, and others.[17,18] Within the polyoxometalate family, vanadates also exhibit a variety of structures and properties, including mixed-valence complexes.[19–21] A plethora of studies have demonstrated that vanadium compounds have a wide array of biological functions and exhibit antibacterial, antiviral, antiparasitic, and antimicrobial properties.[22–24] These compounds are under investigation as a promising class of metal-containing pharmaceutical drugs for the treatment of serious medical conditions, including diabetes[25–29] and cancer.[30,31]

The design and synthesis of vanadium complexes involve the use of organic ligands that possess multiple coordination centres and exhibit the capacity to stabilize vanadium in its highest oxidation state. In this regard, R–CO–NH–NH_2 hydrazides and their corresponding hydrazones are particularly effective. The denticity and functionality exhibited by these

[a]"C. D. Nenitzescu" Institute of Organic and Supramolecular Chemistry of the Romanian Academy, Splaiul Independentei 202B, Bucharest, Romania. E-mail: ddragancea@gmail.com
[b]Institute of Chemistry, Moldova State University, Academy str., 3, MD2028, Chisinau, Republic of Moldova
[c]"Petru Poni" Institute of Macromolecular Chemistry of the Romanian Academy, Aleea Grigore Ghica Vodă 41-A, RO-700487 Iasi, Romania
[d]Department of Chemistry, Biochemistry & Pharmaceutical Sciences, University of Bern, Freiestrasse 3, CH-3012 Bern, Switzerland
[e]Department of Chemistry, Biochemistry & Pharmaceutical Sciences, W. Inäbnit Laboratory for Molecular Quantum Materials, WSS-Research Center for Molecular Quantum Systems, University of Bern, Freiestrasse 3, CH-3012 Bern, Switzerland
[f]Institute of Applied Physics, Moldova State University, Academy str., 5, MD2028, Chisinau, Republic of Moldova. E-mail: svetlana.baca@ifa.usm.md; sbaca_md@yahoo.com

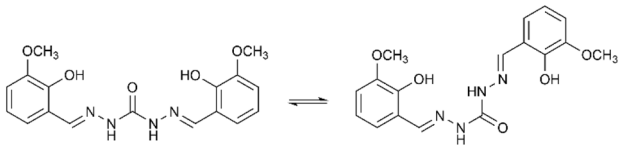

Scheme 1 View of the *syn* (left) and *anti* (right) conformers of the H_4L ligand.

organic compounds can vary depending on the nature of substituents attached to the hydrazone unit. Salicylaldehyde (2-hydroxybenzaldehyde) and its derivatives are advantageous carbonyl precursors for the synthesis of such ligand systems. For instance, symmetrical bis-hydrazones comprising two binding fragments (provided, for example, by an oxalic, adipic, terephthalic central fragment) based on salicylaldehyde and having clearly defined and separated binding sites are widely utilized. The dinuclear[32–34] and polymeric[35] vanadium coordination compounds based on such ligands exhibit high catalytic activity and other useful properties. In this context, a symmetric 1,5-bis(2-hydroxy-3-methoxybenzylidene) carbohydrazide, prepared by the reaction of 2-hydroxy-3-methoxybenzaldehyde (*o*-vanillin) and carbohydrazide, represents a promising ditopic polydentate ligand with multiple potential N,O-donor coordination sites and several coordination clusters based on it have already been reported.[36–38] It is noteworthy that this symmetrical carbohydrazone has the ability to adopt *syn* and *anti* geometric conformations associated with the rotation around a single C–N bond in the amide C(O)–NH fragment (Scheme 1).[39,40]

In continuation of our research on the design and synthesis of carbohydrazone-based coordination compounds,[41,42] we report here new oxidovanadium(v) coordination compounds with the 1,5-bis(2-hydroxy-3-methoxybenzylidene) carbohydrazide (H_4L) ligand. These include the homometallic dinuclear $(NH_4)_2[(VO_2)_2(L)]\cdot 2H_2O$ (**1**) and tetranuclear $[(VO_2)(VO)(EtO)(HL)]_2\cdot 2EtOH$ (**2**) clusters, as well as the heterometallic hexanuclear $[Na_2(H_2O)_4][(VO_2)_4(HL)_2]\cdot 16H_2O$ (**3**) cluster and the $\{[Cs_2(H_2O)_2][(VO_2)_2(L)]\}_n$ (**4**) coordination polymer (Scheme S1). The characterization of compounds **1–4** in the solid state has been conducted through elemental analysis, infrared (IR) spectroscopy, and single-crystal and powder X-ray diffraction studies. These structural determinations in the solid state have been complemented by NMR spectroscopy and ESI-MS spectrometry measurements, which have provided additional insights into molecular conformation of the compounds in solution.

Results and discussion

Spectroscopic and spectrometric characterization

Synthesis. The 1,5-bis(2-hydroxy-3-methoxybenzylidene)carbohydrazide (H_4L) ligand (Scheme 1) has been obtained by the condensation reaction of carbohydrazide with 2-hydroxy-3-methoxybenzaldehyde in a water–ethanol mixture. The reaction of H_4L with NH_4VO_3 in a molar ratio of 1 : 2 in a methanol–ammonium hydroxide solution mixture led to the formation of the dinuclear compound **1**, $(NH_4)_2[(VO_2)_2(L)]\cdot 2H_2O$, with a 78% yield. Compound $[(VO_2)(VO)(EtO)(HL)]_2\cdot 2EtOH$ (**2**) has been prepared by the reaction of $VO(acac)_2$ and H_4L in an ethanol solution, resulting in a yield of 48%. While compound **1** is ionic, consisting of a dinuclear complex $[(VO_2)_2(L)]^{2-}$ anion and two NH_4^+ cations, the tetranuclear complex **2** is neutral. In both cases, solvate water and ethanol molecules are incorporated into the crystal lattices. The introduction of the alkali cations (Na^+ or Cs^+) into the reaction process resulted in the formation of the heterometallic hexanuclear cluster $[Na_2(H_2O)_4][(VO_2)_4(HL)_2]\cdot 16H_2O$ (**3**) in 85% yield, and the coordination polymer $\{[Cs_2(H_2O)_2][(VO_2)_2(L)]\}_n$ (**4**), with yield of 41%.

IR spectroscopy. A comparative analysis of the IR spectra of the ligand and complexes **1–4** (see Fig. S1–S5) showed the following results. Weak broad bands in the 3463–3157 cm^{-1} region in the spectra of compounds **1–4** are attributed to the stretching vibrations of the ν(O–H) and ν(N–H) groups. The absence of the strong ν(C=O) band of amide I at 1665 cm^{-1} in the spectra of the complexes can be explained by the enolization of the carbonyl group and its subsequent coordination. The observed shift of the imine ν(C=N) stretching frequencies to the low-frequency region (1606–1598 cm^{-1}) is attributed to the coordination of the azomethine nitrogen atom to the vanadium(v) atom. All complexes exhibit strong and broad bands centred at 888 (**1**), 871 (**2**), 882 (**3**), and 887 (**4**) cm^{-1}, which are related to the vibrations of the *cis*-VO_2 group.

ESI mass spectrometry. The ESI mass spectrum of **1** in methanol, measured in the negative ion mode, shows peaks at *m*/*z* 521.0 and 535.0, which were assigned to $[(VO_2)_2(HL)]^-$ (10%) and $[(VO_2)(VO)(L)(CH_3O)]^-$ (100%), respectively, fitting the theoretical isotopic distribution patterns well (Fig. S6). The methanolic solution of **2** exhibits signals at *m*/*z* 520.9 and 534.9, which are attributable to the same two ions (Fig. S7). The positive ion mass spectrum of **3** in DMSO shows a base peak corresponding to $\{[(VO_2)_2(L)] + 3Na\}^+$ cations. A peak with 50% relative intensity was well matched with the species of type $\{[(VO_2)_2(L)] + 2Na\}^+$ (Fig. S8). Finally, the positive ion mode spectrum of **4** shows the presence of cations corresponding to $\{[(VO_2)_2(L)] + 2Cs\}^+$ and $\{[(VO_2)_2(L)] + 3Cs\}^+$ at *m*/*z* 786.4 and 918.9, respectively (Fig. S10). All negative mode mass spectra of heterometallic compounds **3** and **4** contain a peak of 100% relative intensity corresponding to the $[(VO_2)_2(HL)]^-$ species (Fig. S9 and S11).

NMR spectroscopy. The NMR spectra of the H_4L ligand and its coordination compounds **1–4** are shown in Fig. S12–S23. The ^1H NMR spectra of **1–4** display characteristic signals of functional groups, as follows: peaks at approx. 3.77–3.74 ppm correspond to the two methoxy groups; aromatic signals appear in the 7.36–6.60 ppm range; and sets of signals around 9.57–9.24 and 8.40–8.55 ppm are assigned to inequivalent aldimine protons (C9H and C7H). These signals reflect the deprotonation of the ligand and the formation of two different sets of binding donor atoms ONN and ONO. The ^1H NMR spectra of **2** (Fig. S17–S19) suggest that the complex retains a dinuclear structure in solution. The dissociation of the tetranuclear cluster **2** in DMSO is supported by mass spectrometry, specifically the peaks at *m*/*z*

520.9 ($[(VO_2)_2(HL)]^-$) and *m*/*z* 534.9 ($[(VO_2)(VO)(L)(CH_3O)]^-$). Furthermore, aliphatic signals for both coordinated EtOH (1.53 for CH_3 and 5.83–5.75 ppm for CH_2), and outer-sphere EtOH (1.05 for CH_3 and 3.43 ppm for CH_2) are observed (Fig. S19). Notably, compounds **3** and **4**, which contain alkali metals, exhibit lower solubility in common organic solvents, with the coordination polymer **4** being the least soluble. While such extended structures typically dissociate in donor solvents, the strong coordination ability of DMSO specifically promotes the cleavage of the polymeric framework into discrete molecular species.

Crystal structures

Dinuclear and tetranuclear V(v) clusters 1 and 2. Compound **1**, $(NH_4)_2[(VO_2)_2(L)]\cdot 2H_2O$, crystallizes in the triclinic space group $P\bar{1}$ (Table S1). The asymmetric unit consists of a dinuclear $[(VO_2)_2(L)]^{2-}$ complex anion, two NH_4^+ cations, and two solvate water molecules. The structure of complex **1** is shown in Fig. 1 and S24. The values of the bond distances in the organic ligand (Table S2) confirm its stabilization in the enolic form.

Within the complex anion, the fully deprotonated hexadentate ligand L^{4-} coordinates to two oxidovanadium(v) ions *via* its ONN and ONO donor sets, resulting in a V⋯V distance of 5.006(2) Å. In **1**, the V1 and V2 atoms are pentacoordinated, exhibiting distorted square-pyramidal N_2O_3 ($\tau = 0.252$) and NO_4 ($\tau = 0.302$) environments, respectively (where $\tau = 0.00$ and 1.00 represent ideal square-pyramidal and trigonal-bipyramidal arrangements[43]). These distorted square-pyramidal geometries (SPY-5) are further supported by SHAPE analysis,[44] which yielded deviation values of 1.858 and 1.105 for V1 and V2, respectively (see Table S4). The V–O bond distances range from 1.881(2) to 1.940(2) Å, while the V–N and V=O bond distances are in the ranges of 2.046(2)–2.199(2) Å and 1.621(2)–1.641(2) Å, respectively (Table S2). The bond distances and valence angles within the coordination polyhedra of the V(v) ions in **1** are comparable to those observed in related vanadium complexes with hydrazone-based ligands.[42,45] In the crystal lattice, the dinuclear anions, NH_4^+ cations and crystallization water molecules participate in N–H⋯O and O–H⋯O intermolecular hydrogen bonds (Table S3), forming a three-dimensional (3D) supramolecular structure, as shown in Fig. S25.

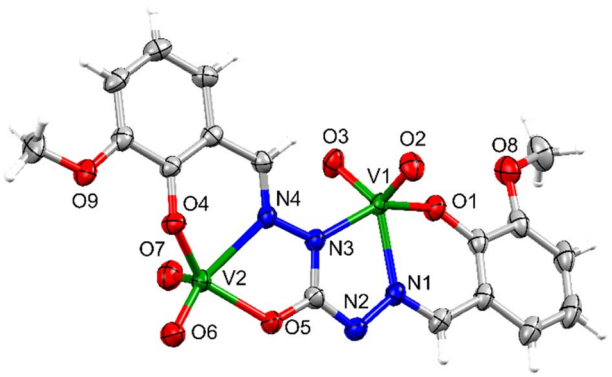

Fig. 1 The structure of $[(VO_2)_2(L)]^{2-}$ anion in **1** with thermal ellipsoids shown at the 50% probability level and partial atom numbering.

Compound **2**, $[(VO_2)(VO)(EtO)(HL)]_2\cdot 2EtOH$, crystallizes in the monoclinic space group $P2_1/c$ (Table S1). The asymmetric unit contains one-half of the centrosymmetric, neutral tetranuclear complex $[(VO_2)_2(VO)_2(HL)_2(EtO)_2]$ and a solvate ethanol molecule (Fig. 2 and S26). The core of the cluster is composed of two VO^{3+} and two VO_2^+ units.

The tetranuclear cluster $[(VO_2)_2(VO)_2(HL)_2(EtO)_2]$ is shown in Fig. 2b. In **2**, the ligand coordinates to the V1 and V2 atoms as a trianionic HL^{3-} species, forming two five-membered and two six-membered chelate rings and adopting a nearly planar configuration with the dihedral angle between the two phenyl rings of 1.620°. The coordination environments of V1 and V2

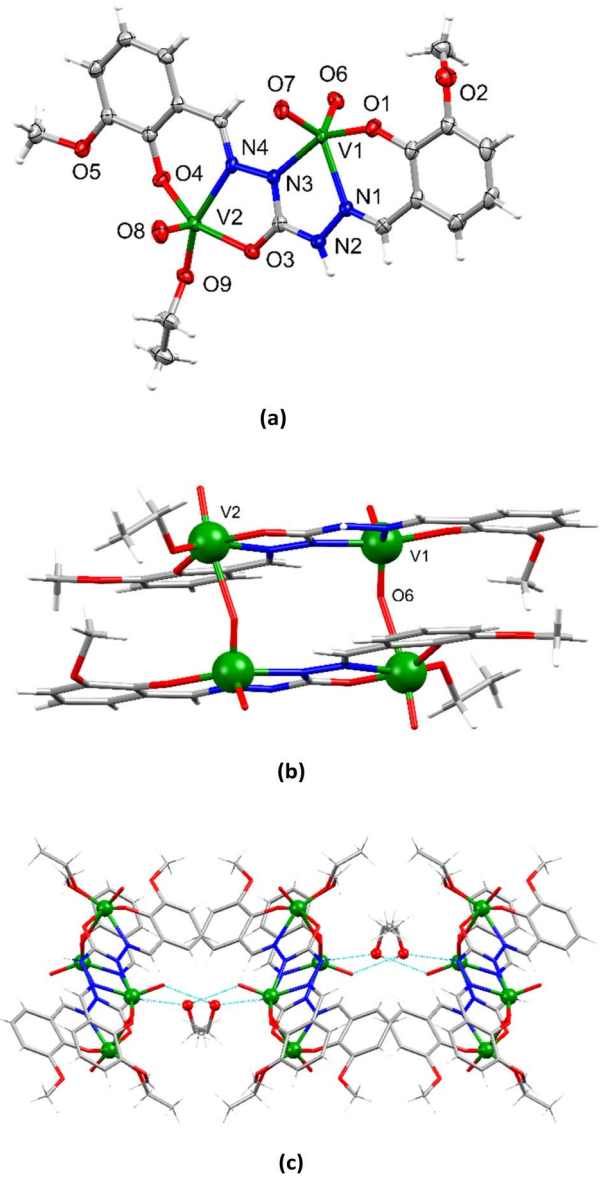

Fig. 2 The asymmetric unit of compound **2** with thermal ellipsoids shown at the 50% probability level (a) and the structure of tetranuclear $[(VO_2)(VO)(HL)(EtO)]_2$ cluster (b) in **2**. Solvent EtOH molecules are omitted for clarity. The supramolecular layer formed in **2** *via* hydrogen bonds between solvent EtOH molecules and tetranuclear V(v) clusters viewed along the *b* axis. Hydrogen bonds are shown as blue dotted lines (c).

atoms in **2** are different. The V1 atom exhibits a pentacoordinate geometry, with an N_2O_3 donor atom set. The calculated τ value was determined to be 0.509, indicating an intermediate position between two geometries, but a slight shift towards trigonal-bipyramidal geometry. The calculation of coordination geometry for the V1 atom, as performed by SHAPE analysis,[44] also indicates a preferable trigonal-bipyramidal configuration (TBPY-5), with a deviation value of 2.946, compared to 3.656 for the square-pyramidal alternative (Table S4).

The V=O bond distances are 1.621(2) and 1.631(2) Å, the V–O bond distance is 1.884(2) Å, and the V–N bond distances equal 2.086(2) and 2.168(2) Å. In contrast, the coordination environment of the V2 atom can be described as a distorted NO_5 octahedral geometry. It is characterized by a displacement of the V2 atom by 0.295(2) Å from the main plane defined by donor atoms N4, O3, O4, and O9 toward the O8 oxido ligand, and a significantly long bond distance of 2.308(2) Å between V2 and O6 (Table S2). This geometry is further confirmed by SHAPE analysis[44] with a deviation value of 1.043 for the octahedral geometry (vOC-5). The remaining V=O and V–O bond distances are 1.590(2) and 1.762(2)–1.983(2) Å, respectively, while the V–N bond distance is 2.169(2) Å. All bond distances for the oxido and dioxidovanadium sites in **2** are in good agreement with those reported for other tetranuclear V(v) compounds.[42] The solvate ethanol molecules function as both donors and acceptors of hydrogen bonds, thereby joining neighbouring tetranuclear clusters *via* O20–H20···O7[$-x, y+1/2, -z+3/2$] = 2.912(2) Å and N2–H2···O20 = 2.769(3) Å to form a supramolecular layer (Fig. 2b and S27).

Hexanuclear Na–V(v) cluster 3. Compound **3**, $[Na_2(H_2O)_4][(VO_2)_4(HL)_2]\cdot 16H_2O$, crystallizes in the monoclinic space group $P2_1/c$. The unit cell contains two crystallographically independent, centrosymmetric, neutral hexanuclear $[Na_2(H_2O)_4][(VO_2)_4(HL)_2]$ clusters, denoted as A and B, along with solvate water molecules (Fig. 3a, b and S28). Similar to **2**, the triply deprotonated HL^{3-} ligand coordinates to two oxidovanadium(v) cations *via* the ONN and ONO donor sets. Two such residues are linked together through the coordination of the methoxy and hydroxy oxygen atoms of the HL^{3-} ligands, as well as one of the oxo-O atoms of the VO_2 cores, to two sodium cations, thereby forming a hexanuclear aggregate as shown in Fig. 3c. This assembly can also be defined as a dimer composed of two dinuclear anionic $[(VO_2)_2(HL)]^-$ units bridged by two $[Na(H_2O)_2]^+$ cations (Fig. S29a).

All vanadium atoms in **3** exhibit a pentacoordinate geometry with a N_2O_3 square-pyramidal configuration (V1A, V1B, and their symmetry-equivalent sites) or a NO_4 square-pyramidal environment (V2A, V2B, and their symmetry-equivalent sites). This ia indicated by τ values of 0.188 (V1A), 0.023 (V2A), 0.132 (V1B), and 0.005 (V2B). The deviation values of 1.740 (V1A), 0.924 (V2A), 1.386 (V1B), and 0.809 (V2B), determined by SHAPE analysis,[44] provide further support for the adoption of a square pyramidal geometry (SPY-5) for all vanadium atoms. The V–O_{HL} bond distances range from 1.880(4) to 1.963(3) Å, while the V–N and V=O bond distances vary between 2.038(3)–2.173(4) Å and 1.617(3)–1.650(4) Å, respectively (Table S2).

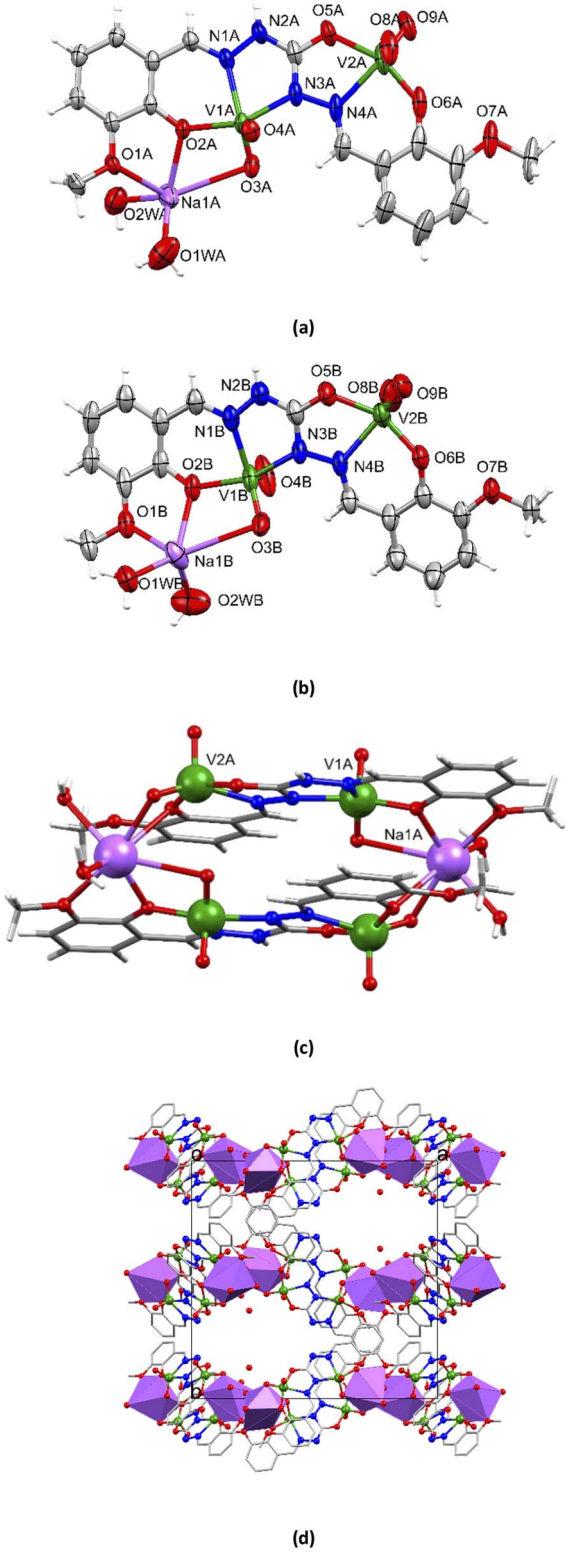

Fig. 3 View of the asymmetric unit of compound **3**, showing one-half of each of the two crystallographically independent, centrosymmetric clusters A (a) and B (b). Atoms are labelled with suffixes A and B respectively. Displacement ellipsoids are shown at the 50% probability level. Structure of the neutral hexanuclear $[Na_2(H_2O)_4][(VO_2)_4(HL)_2]$ cluster, denoted as A in **3** (c). Top view of the crystal packing of hexanuclear V–Na clusters with Na^+ ions shown in polyhedral model in **3**, highlighting the formation of channels filled with water molecules (d).

The coordination environment of the Na^+ ions (Na1A and Na1B, and their symmetry-equivalent sites) consists of three O atoms from two HL^{3-} ligands (Na–O_{HL}, 2.353(4)–2.739(5) Å), and two terminal O atoms (Na–O, 2.425(4)–2.923(4) Å) of the VO_2 core. The heptacoordinated Na^+ ion is complemented by two water molecules, with Na–O bond distances ranging from 2.309(7) to 2.409(6) Å (Table S2). The observed Na–O bond distances are consistent with the bond distances distribution for seven-coordinated Na^+ ions bonded to oxygen.[46] According to SHAPE analysis,[44] Na1A adopts a capped trigonal-prismatic geometry (CTPR-7) with a deviation value of 3.286, whereas Na1B adopts a geometry intermediate between a capped octahedron (COC-7, 3.015) and a capped trigonal prism (CTPR-7, 3.159) (Table S5).

Notably, the coordinated water molecule (O1WB) participates in the formation of hydrogen bonds of 2.796(8) Å with the O atom (O4A) of the VO_2 cores of neighbouring hexanuclear $\{Na_2V_4\}$ clusters, connecting them into one-dimensional (1D) hydrogen-bonded chains (Fig. S29b). The packing of these hexanuclear clusters creates channels filled with highly disordered solvent water molecules, as shown in Fig. 3d. The total potential solvent area of the channels, as calculated by PLATON,[47] amounts to 1559 $Å^3$, which constitutes 25.5% of the unit cell volume.

Cs–V(v) coordination polymer 4. Compound **4**, $\{[Cs_2(H_2O)_2][(VO_2)_2(L)]\}_n$, crystallizes in the *C*2/*c* space group of the monoclinic system (Table S1) and possesses a polymeric structure (Fig. 4 and S30–S31). In **4**, the fully deprotonated L^{4-} ligand coordinates to VO_2^+ and Cs^+ ions through all its O- and N donor atoms, as shown in Fig. S30b. The vanadium-based moieties are interconnected *via* Cs2 atoms to form ribbons (Fig. S31a). Furthermore, the coordinated water molecules, O2W and O3W, and Cs1 atoms link these ribbons into a 3D framework (Fig. 4b and S31b). Similar to compounds **1–3**, all V(v) atoms in **4** exhibit a five-coordinate. However, the V1 and V2 atoms have different geometries. The V1 atom adopts a square-pyramidal environment (τ = 0.138; SHAPE analysis – SPY-5, deviation 0.824), whereas the V2 atom exhibits a trigonal-bipyramidal geometry (τ = 0.521; SHAPE analysis – TBPY-5, deviation 2.433) (Table S4). The V–O bond distances range from 1.622(3) to 1.964(3) Å, and the V–N bond distances equal 2.027(3) and 2.165(3) Å.

Cesium cations in **4** adopt different coordination geometries (Table S5). The Cs1 atom is eight-coordinate, exhibiting a distorted elongated trigonal-bipyramidal $Cs1NO_7$ geometry (ETBPY-8, deviation 13.430), with Cs–O bond distances ranging from 3.038(3) to 3.556(5) Å and a Cs1–N bond distance of 3.505(3) Å. The O2W and O3W atoms, with occupancies of 50% and 33%, respectively (Cs1–O2W, 2.993(2) Å; Cs1–O3W, 3.375(9) Å), contribute to the coordination geometry of Cs1, resulting in a deca-coordinated ($Cs1NO_9$) structure that can be characterized as a pentagonal prism (PPR-10) with a deviation value of 9.163. For Cs2, the $Cs2O_7$ coordination geometry is best described as a Johnson elongated triangular pyramid J7 (JETRY-7, deviation 11.288) (Table S5). The Cs–O bond distances are in the range of 3.083(3)–3.311(3) Å (Table S2).

The experimental powder X-ray diffraction (PXRD) patterns of compounds **1–4** were compared with the simulation results obtained from the single crystal X-ray diffraction data set (see Fig. S32–S35). The results indicate that the single crystals are representative of the bulk microcrystalline materials.

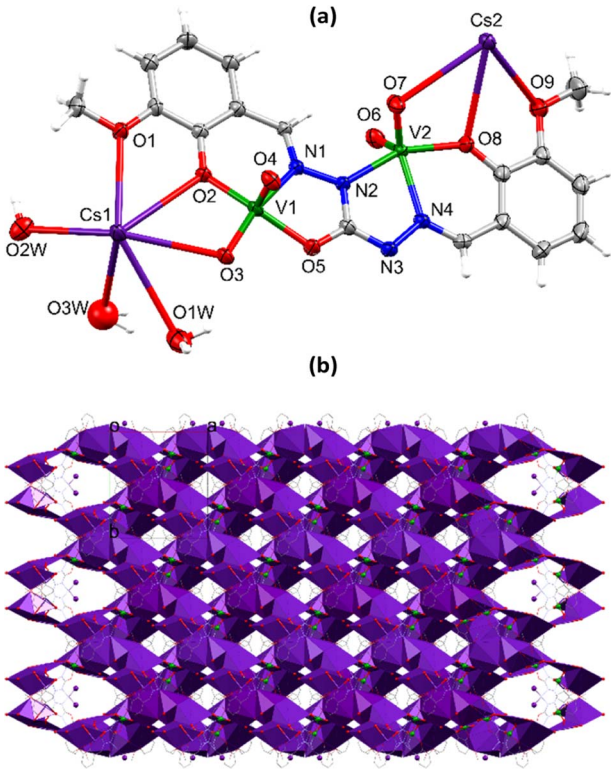

Fig. 4 The asymmetric unit of **4** with thermal ellipsoids shown at the 50% probability level (a). View of the 3D coordination polymer of **4** along the *c* axis, with Cs atom shown in polyhedral design. Hydrogen atoms are omitted for clarity (b).

Experimental

Materials and methods

The chemicals NH_4VO_3, $VO(acac)_2$, 2-hydroxy-3-methoxybenzaldehyde, carbohydrazide, 28% ammonium hydroxide solution, and solvents (ACS reagent) were obtained from commercial sources and were used without further purification. Powder XRD measurements were performed on freshly prepared samples of **1–4** on a RIGAKU MiniFlex 600 diffractometer. IR spectra were recorded on a PerkinElmer FTIR spectrophotometer (H_4L ligand and compounds **1** and **2**) and a Tensor 37 spectrophotometer in the 4000–400 cm^{-1} region (compounds **3** and **4**). ESI mass spectra for compounds **1–4** were recorded on MS spectra Varian 310 – MS LC/MS/MS triple quadrupole mass spectrometer fitted with an electrospray ionization interface (ESI). All NMR (^1H and ^{13}C NMR) measurements were recorded on a Bruker Avance III Ultrashield Plus spectrometer operating at 11.74 T, corresponding to the resonance frequency of 500.13 MHz for the 1H nucleus at 25 °C.

Crystallography

X-ray data sets for compound **1**, **3** and **4** were collected a Rigaku XtaLAB Synergy-S diffractometer, and for **2** on an Oxford Diffraction SuperNova area-detector diffractometer equipped with monochromated Mo Kα radiation. All experimental datasets were processed using the CrysAlisPro software.[48] The structures were solved either by direct methods or an intrinsic phasing approach and refined by full-matrix least-squares on weighted F^2 values for all reflections using the SHELXL suite of programs.[49] The non-hydrogen atoms were refined anisotropically. All H-atoms were placed in geometrically calculated positions and refined using a riding model where each H-atom was assigned a fixed isotropic displacement parameter. The crystal structures **3** contained large areas filled with strongly disordered solvent molecules that could not be modelled using atomic sites, therefore the Mask option of Olex2 (ref. 50) was used to model the contribution of disordered solvent molecules to structure factors. The solvent masked volume constitutes 1559 Å^3 (25.5%) in one void per unit cell, which is consistent with the presence of 13 water molecules per formula unit. In **4**, the cesium cations Cs1 to be disordered over two positions with 0.89/0.11 site occupancies. Crystallographic data and structure refinements of **1–4** are summarized in Table S1, selected bond distances are given in Table S2, and the details of the hydrogen bonding interactions are shown in Table S3. The figures were drawn using the Mercury program.[51]

Crystal data for **1** at 293(2) K: $C_{17}H_{26}N_6O_{11}V_2$, $M_r = 592.32$ g mol^{-1}, 0.2 × 0.05 × 0.05 mm, triclinic, *P*-1, $a = 9.4298(5)$, $b = 10.8957(6)$, $c = 11.9941(8)$ Å, $\alpha = 85.710(5)$, $\beta = 75.669(5)$, $\gamma = 86.699(4)°$, $V = 1189.661(12)$ Å^3, $Z = 2$, 17 723 reflections collected, 5998 independent ($R_{int} = 0.0382$), $R_1 = 0.0377$ and $wR_2 = 0.0980$ [$I > 2$ sigma (I)], $R_1 = 0.0532$ and $wR_2 = 0.1042$ (all data).

Crystal data for **2** at 100(2) K: $C_{42}H_{52}N_8O_{20}V_4$, $M_r = 1192.68$ g mol^{-1}, 0.2 × 0.05 × 0.03 mm, monoclinic, $P2_1/c$, $a = 12.607(3)$, $b = 18.2159(4)$, $c = 10.6813(3)$ Å, $\beta = 93.299(2)°$, $V = 2448.87(11)$ Å^3, $Z = 2$, 14 830 reflections collected, 4666 independent ($R_{int} = 0.0301$), $R_1 = 0.0364$ and $wR_2 = 0.087$ [$I > 2$ sigma (I)], $R_1 = 0.0484$ and $wR_2 = 0.0878$ (all data).

Crystal data for **3** at 200(2) K: $C_{34}H_{70.73}N_8Na_2O_{38.37}V_4$, $M_r = 1455.33$ g mol^{-1}, 0.1 × 0.05 × 0.05 mm, monoclinic, $P2_1/c$, $a = 22.3715(2)$, $b = 21.0369(2)$, $c = 13.4229(12)$ Å, $\beta = 103.7215(9)°$, $V = 6136.92(10)$ Å^3, $Z = 4$, 49 553 reflections collected, 12 155 independent ($R_{int} = 0.0325$), $R_1 = 0.0760$ and $wR_2 = 0.2303$ [$I > 2$ sigma (I)], $R_1 = 0.0850$ and $wR_2 = 0.2399$ (all data).

Crystal data for **4** at 200(2) K: $C_{17}H_{18}Cs_2N_4O_{11}V_2$, $M_r = 821.29$ g mol^{-1}, 0.18 × 0.15 × 0.05 mm, monoclinic, $C2/c$, $a = 16.247(2)$, $b = 16.4323(2)$, $c = 19.9683(2)$ Å, $\beta = 111.623(1)°$, $V = 4955.9(9)$ Å^3, $Z = 8$, 15 673 reflections collected, 4377 independent ($R_{int} = 0.0394$), $R_1 = 0.0332$ and $wR_2 = 0.0906$ [$I > 2$ sigma (I)], $R_1 = 0.0339$ and $wR_2 = 0.0913$ (all data).

Synthetic procedures

The 1,5-bis(2-hydroxy-3-methoxybenzylidene)carbohydrazide (H_4L) was obtained according to a modified procedure previously described in 8. To the solution obtained by dissolving carbohydrazide (0.225 g; 2.5 mmol) in 15 mL of a water–ethanol mixture (1 : 2 by volume), 2-hydroxy-3-methoxybenzaldehyde (0.76 g; 5 mmol) was added and the resulting mixture was kept under reflux for 1 hour. The resulting suspension was filtered off and the precipitate was washed with ethanol and dried in air. Yield: 0.81 g (90%). IR (ν, cm^{-1}): 3228, 3145, 3049, 2999, 2935, 2832, 1665, 1577, 1518, 1460, 1247, 1081, 727.

Synthesis of $(NH_4)_2[(VO_2)_2(L)]\cdot 2H_2O$ (1). The mixture of 1,5-bis(2-hydroxy-3-methoxybenzylidene)carbohydrazide (H_4L) (0.90 g, 0.25 mmol) and NH_4VO_3 (0.059 g, 0.5 mmol) in a methanol : ammonium hydroxide solution (28%) (10 mL, 1 : 1) was stirred at room temperature for 2 h. The resulting suspension was filtered, and the orange microcrystalline precipitate was air-dried. Yield: 0.115 g (78%, 0.194 mmol). Single crystals of **1** suitable for X-ray measurements were obtained by recrystallization of 0.010 g of the precipitate from a methanol–ammonium hydroxide solution (10 mL, 1 : 1). Anal. calcd for $(NH_4)_2[(VO_2)_2(L)]\cdot 2H_2O$ (**1**), $C_{17}H_{26}N_6O_{11}V_2$: C, 34.47; H, 4.42; N, 14.19%. Found: C, 33.94; H, 4.30; N, 13.39%. FT-IR (ν, cm^{-1}): 3463 br.w, 3157 sh, 2981 br.m, 2833 sh, 1606 m, 1558 m, 1523 s, 1454 sh, 1435 vs, 1374 sh, 1356 s, 1292 sh, 1269 sh, 1249 s, 1228 s, 1173 m, 1153 s, 1118 sh, 1106 m, 1095 sh, 1079 m, 1042 m, 975 m, 965 sh, 954 m, 926 sh, 899 sh, 888 vs, 865 s, 771 s, 732 s, 720 s. ^{1}H NMR (500 MHz, DMSO-d_6, δ ppm, J Hz): 9.27 (s, 1H, CH=N), 8.40 (s, 1H, CH=N), 7.01–6.97 (m, 2H, H_{Ar}), 6.89–6.85 (m, 2H, H_{Ar}), 6.73 (t, 1H, H_{Ar}, 7.8 Hz), 6.63 (t, 1H, H_{Ar}, 7.8 Hz), 3.76 (s, 3H, OCH_3), 3.74 (s, 3H, OCH_3) ppm. ^{13}C NMR (125 MHz, DMSO-d_6, δ ppm): 153.2, 149.4, 149.2, 149.0, 143.1, 123.1, 122.8, 121.6, 121.0, 116.6, 115.9, 113.8, 113.7, 113.0, 112.9, 55.7, 55.5 ppm. ESI-MS in methanol (negative): m/z 521.0 $[(VO_2)_2(HL)]^-$ (calcd for $C_{17}H_{15}N_4O_9V_2$: 520.97); m/z 535.0 $[(VO_2)(VO)(L)(CH_3O)]^-$ (calcd for $C_{18}H_{17}N_4O_9V_2$: 534.99).

Synthesis of $[(VO_2)(VO)(EtO)(HL)]_2\cdot 2EtOH$ (2). The mixture of 1,5-bis(2-hydroxy-3-methoxybenzylidene)carbohydrazide (H_4L) (0.045 g, 0.125 mmol) and VO(acac)$_2$ (0.066 g, 0.25 mmol) in EtOH (20 mL) was stirred at room temperature for 2 hours to obtain a brown, cloudy solution, which was filtered and the filtrate was left for slow evaporation. The brown crystals of **2** suitable for single X-ray diffraction analysis were filtered off in two days and dried in air. Yield: 0.036 g (48%, 0.030 mmol). Anal. calcd for $[(VO_2)(VO)(EtO)(HL)]_2\cdot 2EtOH$ (**2**), $C_{42}H_{52}N_8O_{20}V_4$: C, 42.30; H, 4.39; N, 9.40%. Found: C, 42.64; H, 4.73; N, 9.78%. FT-IR (ν, cm^{-1}): 3447 br.m, 3222 sh, 3069 sh, 2971 br.m, 2933 sh, 1601 vs, 1557 s, 1511 s, 1450 sh, 1435 vs, 1380 m, 1363 m, 1251 vs, 1228 s, 1194 sh, 1174 sh, 1097 sh, 1079 m, 1035 m, 948 m, 896 sh, 871 s, 769 m, 733 m, 702 m. ^{1}H NMR (500 MHz, DMSO-d_6, δ ppm, J Hz): 12.66 (s, 1H, NH), 9.57 (s, 1H, CH=N), 8.55 (s, 1H, CH=N), 7.36 (d, 1H, H_{Ar}, 7.4 Hz), 7.25–7.22 (m, 2H, H_{Ar}), 7.15–7.11 (m, 1H, H_{Ar}), 6.91 (t, 1H, H_{Ar}, 7.9 Hz), 6.83–6.80 (m, 1H, H_{Ar}), 5.83–5.75 (m, 2H, CH_2 (Et)), 3.85 (s, 3H, OCH_3), 3.78 (s, 3H, OCH_3), 1.53 (t, 3H, CH_3 (Et), 7.0 Hz) ppm. ESI-MS in methanol (negative): m/z 520.9 $[(VO_2)_2(HL)]^-$ (calcd for $C_{17}H_{15}N_4O_9V_2$: 520.97); m/z 534.9 $[(VO_2)(VO)(L)(CH_3O)]^-$ (calcd for $C_{18}H_{17}N_4O_9V_2$: 534.99).

Synthesis of $[Na_2(H_2O)_4][(VO_2)_4(HL)_2]\cdot 16H_2O$ (3) and $\{[Cs_2(H_2O)_2][(VO_2)_2(L)]\}_n$ (4). To a solution of VO(acac)$_2$ (0.066 g, 0.25 mmol) in acetonitrile (for **3**) or ethanol (for **4**) (5 mL) 1,5-

bis(2-hydroxy-3-methoxybenzylidene)carbohydrazide (H_4L) (0.045 g, 0.125 mmol) was added and the mixture was stirred for 1 hour until a clear brown solution was obtained. To this solution, an aqueous solution (5 mL) of alkali metal carbonate [Na_2CO_3 (0.027 g, 0.25 mmol) for **3**; or Cs_2CO_3 (0.082 g, 0.25 mmol) for **4**] was added, and stirring was continued for another hour. The resulting reddish solution was filtered, then left to crystallize. After 10 days the red-brown crystals of **3** and **4** were filtered off and dried in air.

$[Na_2(H_2O)_4][(VO_2)_4(HL)_2]\cdot 17H_2O$ (3). Yield: 0.063 g (85%, 0.042 mmol). Anal. calcd for **3**, $C_{34}H_{38}N_8Na_2O_{22}V_4\cdot nH_2O$, n = 13: C, 29.28; H, 4.63; N, 8.03%. Found: C, 29.67; H, 4.37; N, 7.92%. IR (ν, cm^{-1}): 3368 br.m, 1598 m, 1560 m, 1506 s, 1471 s, 1441 sh, 1379 sh, 1358 s, 1290 m, 1250 s, 1228 s, 1148 m, 1110 m, 1078 m, 1037 m, 977 sh, 924 sh, 882 vs, 771 m, 734 sh, 639 sh, 606 vs ^{1}H NMR (500 MHz, DMSO-d_6, δ ppm, J Hz): 9.25 (s, 1H, CH═N), 8.40 (s, 1H, CH═N), 7.00–6.96 (m, 2H, H_{Ar}), 6.88–6.85 (m, 2H, H_{Ar}), 6.72 (t, 1H, H_{Ar}, 7.8 Hz), 6.62 (t, 1H, H_{Ar}, 7.8 Hz), 3.76 (s, 3H, CH_3), 3.75 (s, 3H, CH_3) ppm. ^{13}C NMR (125 MHz, DMSO-d_6, δ ppm): 175.3, 153.2, 153.1, 149.4, 149.2, 146.7, 144.7, 123.0, 122.7, 121.7, 121.2, 116.6, 115.8, 113.6, 112.8, 55.7, 55.5 ppm. ESI-MS in DMSO (negative): m/z 521.1 $[(VO_2)_2(HL)]^-$ (calcd for $C_{17}H_{15}N_4O_9V_2$: 520.97). ESI-MS in DMSO (positive): m/z 566.8 $\{[(VO_2)_2(L)] + 2Na\}^+$ (calcd for $C_{17}H_{14}N_4O_9Na_2V_2$: 565.94); m/z 588.9 $\{[(VO_2)_2(L)] + 3Na\}^+$ (calcd for $C_{17}H_{14}N_4O_9Na_3V_2$: 589.2).

$\{[Cs_2(H_2O)_2][(VO_2)_2(L)]\}_n$ (4). Yield: 0.045 g (41%, 0.054 mmol). Anal. calcd for $\{[Cs_2(H_2O)_2][(VO_2)_2(L)]\}_n$ (**4**), $C_{17}H_{18}Cs_2N_4O_{11}V_2$: C, 24.84; H, 2.21; N, 6.82%. Found: C, 24.92; H, 2.39; N, 6.64%. IR (ν, cm^{-1}): 3366 br.m, 1599 m, 1559 m, 1511 s, 1467 s, 1443 sh, 1427 s, 1380 m, 1357 s, 1282 m, 1247 s, 1228 s, 1170, 1157, 1120, 1093, 1034, 977, 942, 928, 887, 866, 768, 733 vs, 721 m, 640 m, 614 s, 590 vs, 523 sh, 472 s, 442 s, 417 vs ^{1}H NMR (500 MHz, DMSO-d_6, δ ppm, J Hz): 9.24 (s, 1H, CH═N), 8.40 (s, 1H, CH═N), 7.00–6.97.00 (m, 2H, H_{Ar}), 6.88–6.85 (m, 2H, H_{Ar}), 6.72 (t, 1H, H_{Ar}, 7.8 Hz), 6.62 (t, 1H, H_{Ar}, 7.8 Hz), 3.76 (s, 3H, OCH_3), 3.74 (s, 3H, OCH_3) ppm. ^{13}C NMR (125 MHz, DMSO-d_6, δ ppm): 153.1, 149.4, 149.2, 123.0, 122.8, 121.7, 121.1, 116.5, 115.9, 113.6, 112.8, 55.6, 55.4 ppm. ESI-MS in DMSO (negative): m/z 521.2 $[(VO_2)_2(HL)]^-$ (calcd for $C_{17}H_{15}N_4O_9V_2$: 520.97). ESI-MS in DMSO (positive): m/z 786.4 $\{[(VO_2)_2(L)] + 2Cs\}^+$ (calcd for $C_{17}H_{14}N_4O_9Cs_2V_2$: 786.0); m/z 918.9 $\{[(VO_2)_2(L)] + 3Cs\}^+$ (calcd for $C_{17}H_{14}N_4O_9Cs_3V_2$: 918.9).

Conclusions

The interaction of the polytopic 1,5-bis(2-hydroxy-3-methoxybenzylidene)carbohydrazide ligand (H_4L) with NH_4VO_3 or $VO(acac)_2$ in an alcohol solution resulted in the formation of the dinuclear or tetranuclear homometallic vanadium(v)-based clusters, $(NH_4)_2[(VO_2)_2(L)]\cdot 2H_2O$ (**1**) and $[(VO_2)(VO)(EtO)(HL)]_2\cdot 2EtOH$ (**2**). In dinuclear cluster **1**, the ligand acts as a tetraanion (L^{4-}) and accommodates two homovalent VO_2 ions, whereas in **2** two different oxido and two dioxidovanadium cores (VO_2 and VO) are incorporated by the two trianion (HL^{3-}) ligands into a tetranuclear assembly *via* long V–O–V bonds. In both clusters, the ligand binds V(v) atoms *via* its ONN or ONO sets of donor atoms. The versatility of the ligand's coordination capabilities is further demonstrated by the introduction of Na^+ and Cs^+ cations into the reaction between $VO(acac)_2$ and H_4L. In the heterometallic hexanuclear cluster $[Na_2(H_2O)_4][(VO_2)_4(HL)_2]\cdot 16H_2O$ (**3**), the ligand additionally involves its methoxy oxygen donor atom in the coordination to Na^+ cations, whereas in $\{[Cs_2(H_2O)_2][(VO_2)_2(L)]\}_n$ (**4**) coordination polymer all O and N donor atoms of the L^{4-} ligand are participated in the coordination to metal centres. The presented work highlights the effectiveness of 1,5-bis(2-hydroxy-3-methoxybenzylidene) carbohydrazide as a versatile polytopic ligand, and the suitability of the oxovanadium(v) and dioxovanadium(v) cores in the development of discrete and extended metal–organic architectures.

Author contributions

DD: conceptualization, chemical synthesis and growth of crystals, analysis of the data, writing of the paper; NT: analysis of the data, chemical synthesis and growth of crystals; SS: data collection and refinement, analysis of the data, generation of images, writing of the paper; AH: formal analysis of the data; SG: data collection and refinement, analysis of the data; SD: conceptualization, analysis of the data, writing of the paper; SL: analysis of the data, writing of the paper; SGB: conceptualization, analysis of the data, generation of images, writing of the paper.

Conflicts of interest

There are no conflicts to declare.

Data availability

CCDC 2495523 (**1**), 2495524 (**2**), 2495525 (**3**), and 2495527 (**4**) contain the supplementary crystallographic data for this paper.[52a–d]

The data supporting this article have been included as part of the supplementary information (SI). The raw PXRD data supporting the findings of this study are available from the corresponding author upon reasonable request. Supplementary information: scheme of synthesis Scheme 1, IR spectra (Fig. S1–S5); ESI-MS isotope patterns (Fig. S6–S11); ^{1}H and ^{13}C NMR spectra (Fig. S12–S23); additional details in the structures of **1–4** (Fig. S24–S31); PXRD patterns (Fig. S32–S35); additional crystallographic and structural details (Tables S1–S3); continuous shape measures (CShM) of the coordination geometries of metal centers in **1–4** (Tables S4 and S5). See DOI: https://doi.org/10.1039/d6ra02540d.

Acknowledgements

S.-X. Liu gratefully acknowledges the support of the Swiss National Science Foundation, grant 200021_204053 and the Sinergia grant CRSII5_213533. S. G. Baca is grateful for the subprogram 011202 financed by the Ministry of Education and Research of R. Moldova and the bilateral project "MultiClust"

(01DK25013 and 25.80013.5007.07GER) supported by the German Federal Ministry of Education and Research (BMBF) and the Moldovan National Agency for Research and Development (NARD). We thank Dr J. Hauser for conducting the X-ray measurements of compound **2**.

Notes and references

1 B. J. Hamstra, G. J. Colpas and V. L. Pecoraro, *Inorg. Chem.*, 1998, **37**, 949.
2 P. M. Reis, J. Armando, L. Silva, J. J. R. Frausto da Silva and A. J. L. Pombeiro, *Chem. Commun.*, 2000, 1845.
3 G. Zampella, P. Fantucci, V. L. Pecoraro and L. De Gioia, *Inorg. Chem.*, 2006, **45**, 7133.
4 C. G. Werncke, C. Limberg, C. Knispel, R. Metzinger and B. Braun, *Chem.–Eur. J.*, 2011, **17**, 2931.
5 V. Kraehmer and D. Rehder, *Dalton Trans.*, 2012, **41**, 5225.
6 G. Zampella, L. Bertini and L. De Gioia, *Chem. Commun.*, 2014, **50**, 304.
7 U. Saha and K. K. Mukherjea, *RSC Adv.*, 2015, **5**, 94462.
8 J. Hartung, *New J. Chem.*, 2025, **49**, 2050.
9 B. Chen, Y. Zeng, J. Sha, H. Li, Y. Zhang, L. Liu and W. Zhang, *Biotechnol. Adv.*, 2026, **87**, 108797.
10 D. J. Rehder, *J. Inorg. Biochem.*, 2000, **80**, 133.
11 S. Ye, F. Neese, A. Ozarowski, D. Smirnov, J. Krzystek, J. Telser, J. H. Liao, C.-H. Hung, W.-C. Chu, Y.-F. Tsai, R.-C. Wang, K.-Y. Chen and H.-F. Hsu, *Inorg. Chem.*, 2010, **49**, 977.
12 A. W. Fay, M. A. Blank, C. C. Lee, Y. Hu, K. O. Hodgson, B. Hedman and M. W. Ribbe, *J. Am. Chem. Soc.*, 2010, **132**, 12612.
13 A. G. J. Ligtenbarg, R. Hage and B. L. Feringa, *Coord. Chem. Rev.*, 2003, **237**, 89.
14 V. Conte, A. Coletti, B. Floris, G. Licini and C. Zonta, *Coord. Chem. Rev.*, 2011, **255**, 2165.
15 M. Sutradhar, L. M. D. R. S. Martins, M. F. C. Guedes da Silva and A. J. L. Pombeiro, *Coord. Chem. Rev.*, 2015, **301–302**, 200.
16 R. R. Langeslay, D. M. Kaphan, C. L. Marshall, P. C. Stair, A. P. Sattelberger and M. Delferro, *Chem. Rev.*, 2019, **119**(4), 2128.
17 P. Hu, P. Hu, T. Duc Vu, M. Li, S. Wang, Y. Ke, X. Zeng, L. Mai and Y. Long, *Chem. Rev.*, 2023, **123**(8), 4353.
18 Ch. Geng, M. Zhang, H. Wei, J. Gu, T. Zhao, H. Guan, Sh. Liang, O. Boytsova, Sh. Dou, Y. Chen, Y. Li and Zh. Tian, *Sol. Energy Mater. Sol. Cells*, 2024, **272**, 112892.
19 T. D. Keene, D. M. D'Alessandro, K. W. Krämer, J. R. Price, D. J. Price, S. Decurtins and C. J. Kepert, *Inorg. Chem.*, 2012, **51**, 9192.
20 M. Aureliano, N. I. Gumerova, G. Sciortino, E. Garribba, C. C. McLauchlan, A. Rompel and D. C. Crans, *Coord. Chem. Rev.*, 2022, **454**, 214344.
21 R. Dinda, E. Garribba, D. Sanna, D. C. Crans and J. Costa Pessoa, *Chem. Rev.*, 2025, **125**(3), 1468.
22 K. H. Thompson and C. Orvig, *Coord. Chem. Rev.*, 2001, **219–221**, 1033.
23 D. Rehder, *Inorg. Chim. Acta*, 2023, **549**, 121387.
24 L. H. Delgado-Rangel, V. Reyes-Márquez, M. E. Moreno-Narváez, A. Aragón-Muriel, J. R. Parra-Unda, J. A. Cruz-Navarro, M. A. Martínez-Torres, H. Valdés and D. Morales-Morales, *New J. Chem.*, 2025, **49**, 3442.
25 D. Sanna, M. Serra, G. Micera and E. Garribba, *Inorg. Chem.*, 2014, **53**, 1449.
26 J. C. Pessoa, S. Etcheverry and D. Gambino, *Coord. Chem. Rev.*, 2015, **301–302**, 24.
27 K. Hashmi, Satya, S. Gupta, A. Siddique, T. Khan and S. Joshi, *J. Trace Elem. Med. Biol.*, 2023, **79**, 127245.
28 L. M. P. F. Amaral, T. Moniz, A. M. N. Silva and M. Rangel, *Int. J. Mol. Sci.*, 2023, **24**, 15675.
29 S. Kumar, S. Kumari, R. Karan, A. Kumar, R. K. Rawal and P. Kumar Gupta, *Inorg. Chem. Commun.*, 2024, **161**, 112014.
30 A. L. de Sousa-Coelho, G. Fraqueza and M. Aureliano, *Pharmaceuticals*, 2024, **17**, 12.
31 N. López-Valdez, A. Gonzalez-Villalva, M. Rojas-Lemus, P. Bizarro-Nevares, B. Casarrubias-Tabarez, M. E. Cervantes-Valencia, M. Ustarroz-Cano, G. Guerrero-Palomo, G. Morales-Ricardes, J. Á. Salgado-Hernández and T. I. Fortoul, *Inorganics*, 2025, **13**, 298.
32 S. Gupta, M. V. Kirillova, M. F. Guedes da Silva and A. J. L. Pombeiro, *Appl. Catal., A*, 2013, **460–461**, 82.
33 M. Sutradhar, N. V. Shvydkiy, M. F. C. G. Guedes da Silva, M. V. Kirillova, Yu. N. Kozlov, A. J. L. Pombeiro and G. B. Shul'pin, *Dalton Trans.*, 2013, **42**, 11791.
34 N. Asghari Lalami, H. Hosseini Monfared, H. Noei and P. Mayer, *Transition Met. Chem.*, 2011, **36**, 669.
35 S. Gupta, M. V. Kirillova, M. F. C. Guedes da Silva, A. J. L. Pombeiro and A. M. Kirillov, *Inorg. Chem.*, 2013, **52**, 8601.
36 C.-J. Kuo, R. J. Holmberg and P.-H. Lin, *Dalton Trans.*, 2015, **44**(46), 19758.
37 H. Ke, S. Zhang, X. Li, Q. Wei, G. Xie, W. Wang and S. Chen, *Dalton Trans.*, 2015, **44**(48), 21025.
38 E. Topic, J. Pisk, D. Agustin, M. Jendrlin, D. Cvijanovic, V. Vrdoljak and M. Rubcic, *New J. Chem.*, 2020, **44**(19), 8085.
39 M. M. Sow, O. Diouf, M. Seck, A. H. Barry and M. Gaye, *Acta Crystallogr.*, 2014, **E70**, o423.
40 N. Talmaci, D. Dragancea, E. Gorincioi, P. Bourosh and V. Kravtsov, *Chem. J. Mold.*, 2023, **18**(2), 53.
41 D. Dragancea, S. Shova, E. A. Enyedy, M. Breza, P. Rapta, L. M. Carrella, E. Rentschler, A. Dobrov and V. B. Arion, *Polyhedron*, 2014, **80**, 180.
42 D. Dragancea, N. Talmaci, S. Shova, G. Novitchi, D. Darvasiova, P. Rapta, M. Breza, M. Galanski, J. Kozısek, N. M. R. Martins, L. M. D. R. S. Martins, A. J. L. Pombeiro and V. B. Arion, *Inorg. Chem.*, 2016, **55**, 9187.
43 A. G. Blackman, E. B. Schenk, R. E. Jelley, E. H. Krenske and L. R. Gahan, *Dalton Trans.*, 2020, **49**, 14798.
44 (*a*) M. Llunell, D. Casanova, J. Cirera, P. Alemany and S. Alvarez, *SHAPE 2.0*, Universitat de Barcelona, Barcelona, 2010; (*b*) S. Alvarez, P. Alemany, D. Casanova, J. Cirera, M. Llunell and D. Avnir, *Coord. Chem. Rev.*, 2005, **249**, 1693.
45 H. Hosseini-Monfared, R. Bikas, P. Mahboubi-Anarjan, S. Weng Ng and E. R. T. Tiekink, *Z. Anorg. Allg. Chem.*, 2014, **640**, 243.

46 O. Gagne and F. Hawthorne, *Acta Crystallogr.*, 2016, **B72**, 602.
47 A. L. Spek, *Acta Crystallogr., Sect. D: Biol. Crystallogr.*, 2009, **D65**, 148.
48 Agilent, *CrysAlis PRO*, Agilent Technologies Ltd, Yarnton, Oxfordshire, England, 2014.
49 G. M. Sheldrick, *Acta Crystallogr.*, 2015, **C71**, 3.
50 O. V. Dolov, L. J. Burkhis, R. J. Gildea, J. A. K. Howard and H. Pushmann, *J. Appl. Crystallogr.*, 2009, **42**(3), 352.
51 C. F. Macrae, I. Sovago, S. J. Cottrell, P. T. A. Galek, P. McCabe, E. Pidcock, M. Platings, G. P. Shields, J. S. Stevens, M. Towler and P. A. Wood, *J. Appl. Crystallogr.*, 2020, **53**, 226.
52 (*a*) CCDC 2495523: Experimental Crystal Structure Determination, 2026, DOI: 10.5517/ccdc.csd.cc2prsr0; (*b*) CCDC 2495524: Experimental Crystal Structure Determination, 2026, DOI: 10.5517/ccdc.csd.cc2prss1; (*c*) CCDC 2495525: Experimental Crystal Structure Determination, 2026, DOI: 10.5517/ccdc.csd.cc2prst2; (*d*) CCDC 2495527: Experimental Crystal Structure Determination, 2026, DOI: 10.5517/ccdc.csd.cc2prsw4.